

Recognition elements that determine affinity and sequence-specific binding to DNA of 2QN, a biosynthetic bis-quinoline analogue of echinomycin

Christian Bailly, Susana Echepare¹, Federico Gago¹ and Michael J. Waring²

Laboratoire de Pharmacologie Antitumorale du Centre Oscar Lambret and U-524 INSERM, IRCL, Place de Verdun, 59045 Lille, France, ¹Departamento de Farmacología, Universidad de Alcalá, 28871 Alcalá de Henares, Madrid, Spain and ²Department of Pharmacology, University of Cambridge, Tennis Court Road, Cambridge CB2 1QJ, UK

Summary

Footprinting experiments with DNase I provide a starting-point for investigating the molecular basis of nucleotide sequence recognition by 2QN, a bis-quinoline derivative of the quinoxaline antibiotic echinomycin produced by directed biosynthesis in *Streptomyces echinatus*. Using *tyrT* DNA molecules variously substituted with inosine and/or 2,6-diaminopurine residues it is shown that the location of the 2-amino group of purine nucleotides in the minor groove of the double helix exerts a dominant influence in determining where the antibiotic will bind, as it does for echinomycin. However, newly created binding sites in DNA molecules substituted with diaminopurine (D), all located round TpD steps, bind 2QN with so much higher affinity than the canonical CpG steps that the latter fail completely to appear as footprints in D-substituted DNA; indeed CpG sequences appear in regions of enhanced susceptibility to nuclease cleavage as do CpI steps in doubly D+I-substituted DNA. Quantitative footprinting plots confirm that sequences surrounding TpD steps bind 2QN several hundred-fold more tightly than do CpG-containing sequences, with dissociation constants of the order of 25 nM. To test the hypothesis that differences in stacking interactions between the chromophores of the drug and the DNA base pairs could account for the differences in binding affinities, models of 2QN bound to two DNA hexamers containing either a central CpG or a central TpD step were built. Calculation of the molecular electrostatic potential (MEP) of 2QN in solution using a continuum method revealed a distinctive pattern that is considered relevant to DNA binding. When the MEPs calculated for the two DNA hexamers in the complexed state were compared, substantial differences were found in the major groove and in the space between the base pairs that is occupied by the chromophores of the drug upon binding.

The modelling data support the notion that electrostatic stacking interactions underlie the considerably preferred binding of echinomycin and 2QN around TpD steps rather than CpG steps.

Key words

DNA binding/echinomycin/footprinting/minor groove recognition/molecular modelling/sequence specificity/2QN/quinoxaline antibiotics

Introduction

Quinoxaline antibiotics, secondary metabolites produced by several species of streptomycetes, were first described in the 1950s, but did not attract much attention as potential anti-cancer drugs until echinomycin, the best-known member of the group, was identified as the first known DNA bis-intercalator some 20 years later (Waring and Wakelin, 1974). The early history of these antibiotics has been summarized by Katagiri *et al.* (1975) and Waring (1979). Nevertheless, although little was known about the mechanism of action of quinoxalines, already in the 1960s heroic efforts were being made to obtain new antibiotics with improved properties by the process of directed biosynthesis in which potential mimetics of the natural quinoxaline ring system are added to cultures of producing microorganisms (Yoshida *et al.*, 1968).

The naturally-occurring antibiotics fall into two series, triostins and quinomycins, which differ in the nature of the sulphur-containing cross-bridge that spans their heterodetic cyclic octadepsipeptide ring (Figure 1). In quinomycins such as echinomycin (quinomycin A) the cross-bridge is a thioacetal, whereas in triostins it is a simple disulphide. Triostins are the immediate biosynthetic precursors of quinomycins, the conversion being effected by enzymic methylation at the expense of *S*-adenosyl-methionine (Cornish *et al.*, 1983a). Within each series of antibiotics, different members vary in respect of the amino acid between *L-N*-methylcysteine and *D*-serine; it is most often *L-N*-methylvaline but it may be

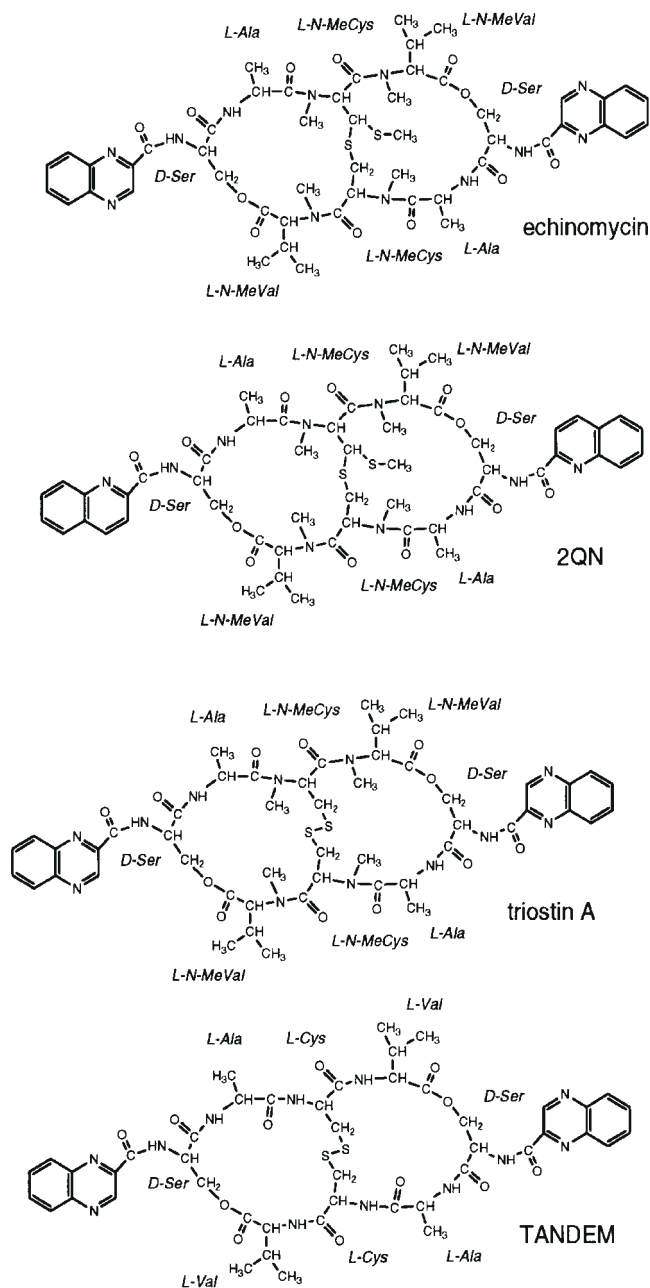


Figure 1
Chemical structure of quinomycin antibiotics.

replaced by one of a small number of other hydrophobic aliphatic amino acids such as *N*- γ -dimethyl-*allo*-isoleucine. Nothing else varies in nature, but numerous other peptide ring variants in the triostin series have been prepared by total synthesis and have yielded valuable information about the DNA-binding properties of these compounds (Lee and Waring, 1978; Fox *et al.*, 1980a, 1982; Olsen *et al.*, 1986; Waring, 1993).

The first reported analogues of quinomycin and triostin containing substituted chromophores, produced by directed biosynthesis, were the mono- and bis-quinoline derivatives of

echinomycin designated 1QN and 2QN respectively, obtained by supplementing cultures of streptomycetes with quinoline-2-carboxylic acid (Yoshida *et al.*, 1968; Gauvreau and Waring, 1984a,b). Subsequently many more analogues containing unnatural chromophores were prepared and examined for DNA binding, but few were selected for biological evaluation because of their poor solubility in aqueous media (Bojesen *et al.*, 1981; Williamson *et al.*, 1982; Cornish *et al.*, 1983b; Santikarn *et al.*, 1983; Cornish *et al.*, 1985). Some of them displayed notably altered DNA-binding characteristics (Fox *et al.*, 1980b; Cornish *et al.*, 1983b; Low *et al.*, 1986). 2QN attracted especial interest because it formed good crystals which were suitable for X-ray diffraction and eventually yielded the only high-resolution structure available for any antibiotic in the quinomycin (echinomycin) series (Sheldrick *et al.*, 1995). Moreover, the physical behaviour of 2QN in ODMR studies (Alfredson *et al.*, 1991a,b) led to a correlation between spectroscopic and thermodynamic properties which is rarely encountered, namely a linear variation of the zero field splitting *D*-parameter of the intercalated aromatic residue with the free energy of DNA binding, suggesting that the DNA sequence-selectivity of quinomycin drugs may largely be controlled by the intercalated ring systems rather than the peptide moiety as is commonly supposed (Maki *et al.*, 1992), a conclusion hinted at in the original binding experiments (Fox *et al.*, 1980b). Yet when footprinting experiments became available to probe the nucleotide sequence-selectivity of 2QN, no great differences from echinomycin were found; both appeared specific for CpG steps with some preference for alternating pyrimidine-purine sequences containing flanking AT base pairs (Low *et al.*, 1986). Modelling studies, on the other hand, have suggested a possible role for stacking interactions between the intercalated quinomycin ring and the DNA base pairs in both modulation of the binding specificity (Gallego *et al.*, 1994) and conformational preferences of the base pairs flanking the bisintercalation site (Gallego *et al.*, 1993).

In the light of recent advances in footprinting methodology (Dabrowiak and Goodisman, 1989; Dabrowiak *et al.*, 1992; Herman *et al.*, 1998) it seemed appropriate to look more closely at the sequence-selectivity of 2QN and to take advantage of the availability of substituted DNA species to investigate molecular determinants of its selectivity as has been done for a wide variety of DNA-binding antibiotics and drugs (Bailly and Waring, 1995a, 1998a). Here we report the results of that exercise, which reveal quantitative differences from echinomycin but complete agreement that the overriding determinant of preferred 2QN binding sites is the 2-amino group of purine nucleotides exposed in the minor groove of the DNA double helix. The basis of such preference has been explored by molecular modelling techniques and theoretical calculations.

Materials and methods

Antibiotic

2QN was prepared from cultures of *Streptomyces echinatus* supplemented with quinoline-2-carboxylic acid (Gauvreau and Waring, 1984a). It was quantitated by disc agar diffusion assay (Gauvreau and Waring, 1982), isolated by solvent extraction and chromatography, characterized and analysed for purity as previously described (Gauvreau and Waring, 1984b).

Chemicals and biochemicals

Ammonium persulphate, Tris base, acrylamide, bis-acrylamide, ultrapure urea, boric acid, tetramethylethylenediamine and dimethyl sulphate were purchased from Merck (Nogent-sur-Marne, France). Formic acid, piperidine and formamide were from Aldrich (L'Isle d'Abeau Chesnes, France). Bromophenol blue and xylene cyanol were from Serva. The nucleoside triphosphate labelled with [γ - 32 P]ATP was obtained from Amersham (Amersham, Bucks, UK). Restriction endonucleases *EcoRI* and *AvaI* (Boehringer, Mannheim, Germany), *Taq* polymerase (Promega, Charbonnières, France), DNase I (Sigma, L'Isle d'Abeau Chesnes, France) and T4 polynucleotide kinase (Pharmacia, Uppsala, Sweden) were each used according to the supplier's recommended protocol in the activity buffer provided. The primers 5'-AATTCCGGTTACCTTTAATC and 5'-TCG-GGAACCCCCACACGGG, having a 5'-OH or 5'-NH₂ terminal group, were obtained from the Laboratory of Molecular Biology, Medical Research Council, Cambridge, UK. Checks were carried out to ensure that the primers blocked with a 5'-NH₂ group were free from contaminants and could not be labelled by the kinase. All other chemicals were analytical grade reagents, and all solutions were prepared using doubly deionized, Millipore filtered water.

Preparation, purification and labelling of DNA fragments containing natural and modified nucleotides

Plasmid pKmp27 (Drew *et al.*, 1985) was isolated from *Escherichia coli* by a standard sodium dodecyl sulphate-sodium hydroxide lysis procedure and purified by banding in CsCl-ethidium bromide gradients. Ethidium was removed by several isopropanol extractions followed by exhaustive dialysis against Tris-EDTA buffer. The purified plasmid was then precipitated and resuspended in appropriate buffer prior to cleavage by the restriction enzymes. The 160 bp *tyrT*(A93) fragment for use as a template was isolated from the plasmid by digestion with restriction enzymes *EcoRI* and *AvaI*. It is worth mentioning that this template DNA bore a 5'-phosphate due to the action of *EcoRI* and thus only the newly synthesized DNA (with normal or modified nucleotides) can be labelled by the kinase.

Polymerase chain reaction (PCR) and DNA labelling

The protocol used to incorporate inosine and/or 2,6-diaminopurine residues into DNA is comparable to those

previously used to incorporate 7-deazapurine or inosine residues with only a few minor modifications (Marchand *et al.*, 1992; Sayers and Waring, 1993; Bailly and Waring, 1995a). PCR reaction mixtures contained 10 ng of *tyrT*(A93) template, 1 μ M each of the appropriate pair of primers (one with a 5'-OH and one with a 5'-NH₂ terminal group) required to allow 5'-phosphorylation of the desired strand, 250 μ M of each appropriate dNTP (dTTP, dCTP plus dATP or dTTP and dGTP or dTTP according to the desired DNA), and 5 units of *Taq* polymerase in a volume of 50 μ l containing 50 mM KCl, 10 mM Tris-HCl, pH 8.3, 0.1% Triton X-100, and 1.5 mM MgCl₂. To prevent unwanted primer-template annealing before the cycles began, the reactions were heated to 60°C prior to adding the *Taq* polymerase. Finally, paraffin oil was added to each reaction to prevent evaporation. After an initial denaturing step of 3 min at 94°C, 20 amplification cycles were performed, each cycle consisting of the following segments: (i) for normal, U-DNA and DAP-DNA, 94°C for 1 min, 37°C for 2 min and 72°C for 10 min; (ii) for I-DNA and I+DAP-DNA, 84°C for 1 min, 30°C for 2 min and 62°C for 10 min. After the last cycle, the extension segment was continued for an additional 10 min at 62 or 72°C, followed by a 5 min segment at 55°C and a 5 min segment at 37°C. The purpose of these final segments was to maximize annealing of full-length product and to minimize annealing of unused primer to full-length product. The reaction mixtures were then extracted with chloroform to remove the paraffin oil, and parallel reactions were pooled. Several extractions with *n*-butanol were performed to reduce the volume prior to loading the samples on to a 6% non-denaturing polyacrylamide gel. After electrophoresis for ~1 h, a thin section of the gel was stained with ethidium bromide so as to locate the band of DNA under UV light. The same band of DNA free from ethidium was excised, crushed and soaked in elution buffer (500 mM ammonium acetate, 10 mM magnesium acetate) overnight at 37°C. This suspension was filtered through a Millipore 0.22 μ m filter and the DNA was precipitated with ethanol. Following washing with 70% ethanol and vacuum drying of the precipitate, the purified DNA was resuspended in the kinase buffer. The purified PCR products were 5'-end labelled with [γ - 32 P]ATP in the presence of T4 polynucleotide kinase according to a standard procedure for labelling blunt-ended DNA fragments. After completion of the reaction the nucleic acid was again purified by 6% polyacrylamide gel electrophoresis and extracted from the gel as described above. Finally, the labelled DNA was resuspended in 10 mM Tris-HCl buffer, pH 7.0, containing 10 mM NaCl.

DNase I footprinting

Routine experiments were performed essentially as described recently (Bailly and Waring, 1995b). The digestion of the samples (6 μ l) of the labelled DNA fragment dissolved in 10 mM Tris buffer (pH 7.0) containing 10 mM NaCl was

initiated by adding 2 μl of a DNase I solution whose concentration had been adjusted to yield a final enzyme concentration of ~ 0.01 units/ml in the reaction mixture. The extent of digestion was limited to $<30\%$ of the starting material so as to minimize the incidence of multiple cuts in any strand ('single-hit' kinetic conditions). Optimal enzyme dilutions were established in preliminary calibration experiments. After 3 min, the digestion was stopped by freeze drying, samples were lyophilized, washed once with 50 μl of water, lyophilized again and then resuspended in 4 μl of an 80% formamide solution containing tracking dyes. Samples were heated at 90°C for 4 min and chilled in ice for 4 min prior to electrophoresis.

Electrophoresis and autoradiography

DNA cleavage products were resolved by polyacrylamide gel electrophoresis under denaturing conditions (0.3 mm thick, 8% acrylamide containing 8 M urea) capable of resolving DNA fragments differing in length by one nucleotide. Electrophoresis was continued until the bromophenol blue marker had run out of the gel (~ 2.5 h at 60 W, 1600 V in TBE buffer, BRL sequencer model S2). Gels were soaked in 10% acetic acid for 15 min, transferred to Whatman 3MM paper, dried under vacuum at 80°C , and subjected to autoradiography at -70°C with an intensifying screen. Exposure times of the X-ray films (Fuji R-X) were adjusted according to the number of counts per lane loaded on each individual gel (usually 24 h).

Quantitation by storage phosphor imaging

A Molecular Dynamics 425E PhosphorImager was used to collect data from storage screens exposed to the dried gels overnight at room temperature (Johnston *et al.*, 1990). Baseline-corrected scans were analysed by integrating all the densities between two selected boundaries using ImageQuant version 3.3 software. Each resolved band was assigned to a particular bond within the *tyrT*(A93) fragment by comparison of its position relative to sequencing standards generated by treatment of the DNA with formic acid followed by piperidine-induced cleavage at the purine residues (G+A track), taking into account the difference in mobility of the standards due to their being one nucleotide shorter and bearing an additional 3' phosphate group which causes them to migrate ~ 1 – 1.5 bands faster than their counterparts generated by DNase I cleavage. Footprinting data are presented in the form $\ln(f_a) - \ln(f_c)$ representing the differential cleavage at each bond relative to that in the control (f_a is the fractional cleavage at any bond in the presence of the drug and f_c is the fractional cleavage of the same bond in the control). The results are displayed on a logarithmic scale for the sake of convenience; positive values indicate enhanced cleavage whereas negative values indicate blockage. Footprinting plots were then constructed by plotting R versus c , where c is the ligand concentration. The relative band intensity R corresponds to the ratio I_c/I_0 ; where I_c is the intensity of the

band at a given ligand concentration c and I_0 is the intensity of the same band in the control lane, i.e. in the absence of the antibiotic (Dabrowiak and Goodisman, 1989; Sayers and Waring, 1993; Bailly *et al.*, 1995).

Model building and energy-minimization of the complexes

The models previously built for echinomycin bound to DNA hexamers containing a central CpG or TpD step were used for modelling the complexes of 2QN with $d(\text{GACGTC})_2$ and $d(\text{GDTDTTC})_2$, which were refined using the same procedure as reported (Gallego *et al.*, 1994). Point charges for the quinoline chromophore of 2QN were calculated by fitting the quantum mechanical molecular electrostatic potential (MEP), calculated *ab initio* using a 6-31G* basis set, to a monopole–monopole expression (Frisch *et al.*, 1995). MEPs in solution were computed by treating the solvent as a continuous dielectric and solving the non-linear Poisson–Boltzmann equation by means of a finite difference method (Gilson *et al.*, 1988), as implemented in the DelPhi module of the Insight II software (Molecular Simulations Inc., 1997). The boundary between the solvent ($\epsilon = 80$) and each solute molecule ($\epsilon = 2$) was defined by the solvent-accessible surface using a probe radius of 1.4 Å. The salt concentration was set to 0.145 M, and the ion radius for the Stern layers was 2 Å. Identical cubic grids centred on the superimposed molecular complexes were used to calculate the MEP around the drug in the bound conformation and around each DNA molecule in the absence of ligand. For the first grid (1.0 Å resolution), a separation of 20 Å was left between any solute atom and the borders of the box and the potentials at the boundaries were calculated analytically by treating each atom as a Debye–Hückel sphere (Klapper *et al.*, 1986). The accuracy of the calculated electrostatic potentials was subsequently improved by defining two smaller boxes (15 and 10 Å separation), each with a lower grid resolution (0.75 and 0.5 Å spacing respectively) so that the new boundary potentials were linearly interpolated from those calculated in the previous run (Gilson *et al.*, 1988). In order to highlight the most dissimilar MEP regions in the DNA molecules, the energy values at each grid point obtained for $d(\text{GDTDTTC})_2$ were subtracted from the values at the same point of the grid obtained for $d(\text{GACGTC})_2$.

Results

Four homologous 160 bp *tyrT* DNA fragments were synthesized by PCR amplification, each containing either natural bases, or inosine residues in place of guanosines (G \rightarrow I substitution), or 2,6-diaminopurine residues (henceforth abbreviated as DAP or D within a sequence for clarity) in place of adenines (A \rightarrow DAP substitution), or both I and DAP residues (Figure 2). In each case, primers in which the 5' terminal nucleotide residue bore a 5'-OH or a 5'-NH₂ terminal group were used so as to enable selective labelling of

one or the other strand in the PCR product, i.e. the Watson (antisense) strand or the Crick (sense) strand chosen at will. The cleavage patterns of the various modified DNAs were analysed and compared to normal DNA using bovine pancreatic DNase I which is much the best probe for footprinting as regards sensitivity, accuracy and ease of handling (Bailly and Waring, 1995b).

The various base substitutions were all found to affect the binding of 2QN to DNA. As shown in Figure 3, addition of 2QN to *tyrT* DNA containing the canonical base pairs (normal DNA) prevents DNase I from cleaving particular sequences which appear as footprints around nucleotide positions 35, 60, 80 and 110. As expected, the same footprints were detected when the DNA substrate was labelled on one or the other of the complementary strands. The replacement of all guanosines by inosine residues practically abolishes the sequence-specific binding process, indicating that the removal of the 2-amino group is detrimental to the binding of 2QN to DNA. This is in accordance with previous results obtained with the natural antibiotics echinomycin and triostin A, which also fail to bind to DNA lacking the purine 2-amino group (Marchand *et al.*, 1992; Bailly and Waring, 1998b). The inosine DNA fails to show footprints even at 25–50 μM , though some non-specific attenuation of nuclease cleavage may be apparent at 75 μM . In sharp contrast, it can be seen at a glance that the two DAP-containing DNA species (A \rightarrow D substitution with or without inosine) provide very good substrates for 2QN. On the Watson strand a particularly strong footprint can be identified around nucleotide position 88. At this position in DAP DNA the newly created binding site is flanked by regions where the cleavage by the enzyme is massively enhanced in the presence of the antibiotic. Clearly the DAP DNA contains highly preferred binding sites for 2QN as well as sequences to which the drug refuses to bind.

It is also apparent from the gel that the minimal drug concentration required to detect footprints on DAP DNA is considerably lower than is needed with DNA containing just the natural bases. As shown in Figure 3 and in previous studies (Low *et al.*, 1986), a 2QN concentration of $\sim 10 \mu\text{M}$ is needed to produce strong footprints at CpG sites in natural DNA. With DAP DNA, the footprint around position 88 is already very pronounced at only 5 μM 2QN (Figure 3). A full titration of the DAP-substituted DNAs with a wide range of concentrations of the antibiotic (Figure 4) reveals that the binding to this newly created site can be unambiguously detected at a concentration as low as 25 nM, i.e. several hundred times lower than that required to detect binding to the best sites in normal DNA. There is no doubt that the A \rightarrow D substitution potentiates the interaction of 2QN with DNA considerably.

In Figure 5 are plotted examples of the concentration-dependence of antibiotic effects on DNA containing DAP residues versus the normal DNA. It can be seen that the C_{50}

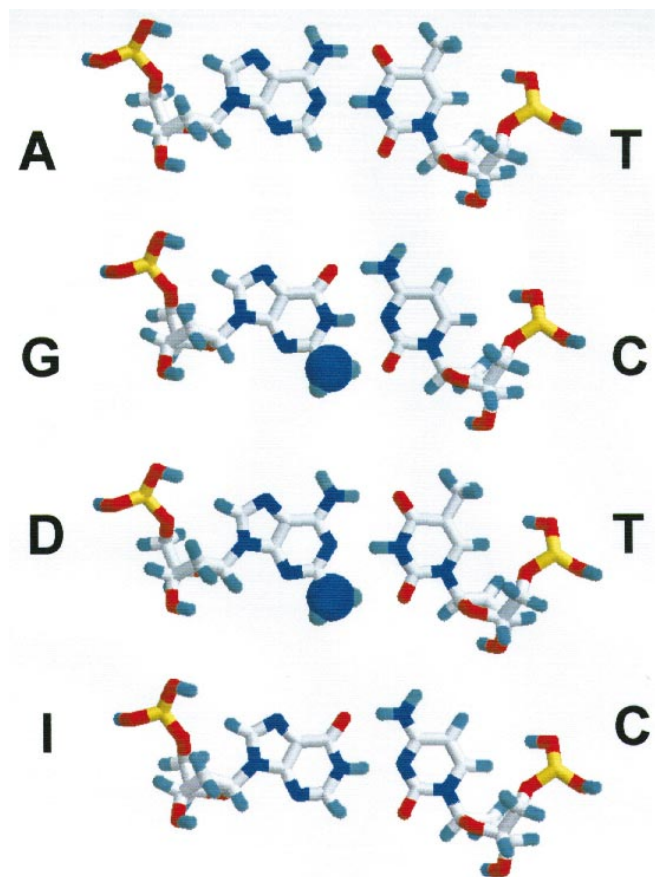


Figure 2

Structures of hydrogen-bonded purine–pyrimidine base pairs. Broken lines represent hydrogen bonds. I and DAP represent inosine and 2,6-diaminopurine (2-aminoadenine) respectively. The purine 2-amino group is shown as a blue sphere.

value (the concentration producing half-maximal effect) for binding of 2QN to the TpD site at position 88 is on the order of 20 nM, whereas for the binding of 2QN to the canonical CpG site at position 76 the C_{50} value is $>8 \mu\text{M}$. This would correspond to a 400-fold increase in affinity for 2QN binding to a TpD site compared to a CpG site in natural DNA. It is worth noting that under the conditions of these footprinting experiments a large fraction of the ligand must be free, so that C_{50} values will approximate to dissociation constants for binding to individual sites (Goodisman and Dabrowiak, 1992; Goodisman *et al.*, 1992).

The sites in the DAP-containing DNA which appear more susceptible to cleavage by DNase I in the presence of 2QN always correspond to GC-rich steps. For instance, the cleavage by the nuclease at CpG 76 in DAP DNA appears considerably increased in the presence of the drug, and again the enhancement of cleavage at this position occurs with half-maximal effect at $\sim 80 \text{ nM}$. The enhanced cleavage at TpA 88 in normal DNA occurs for 2QN concentrations

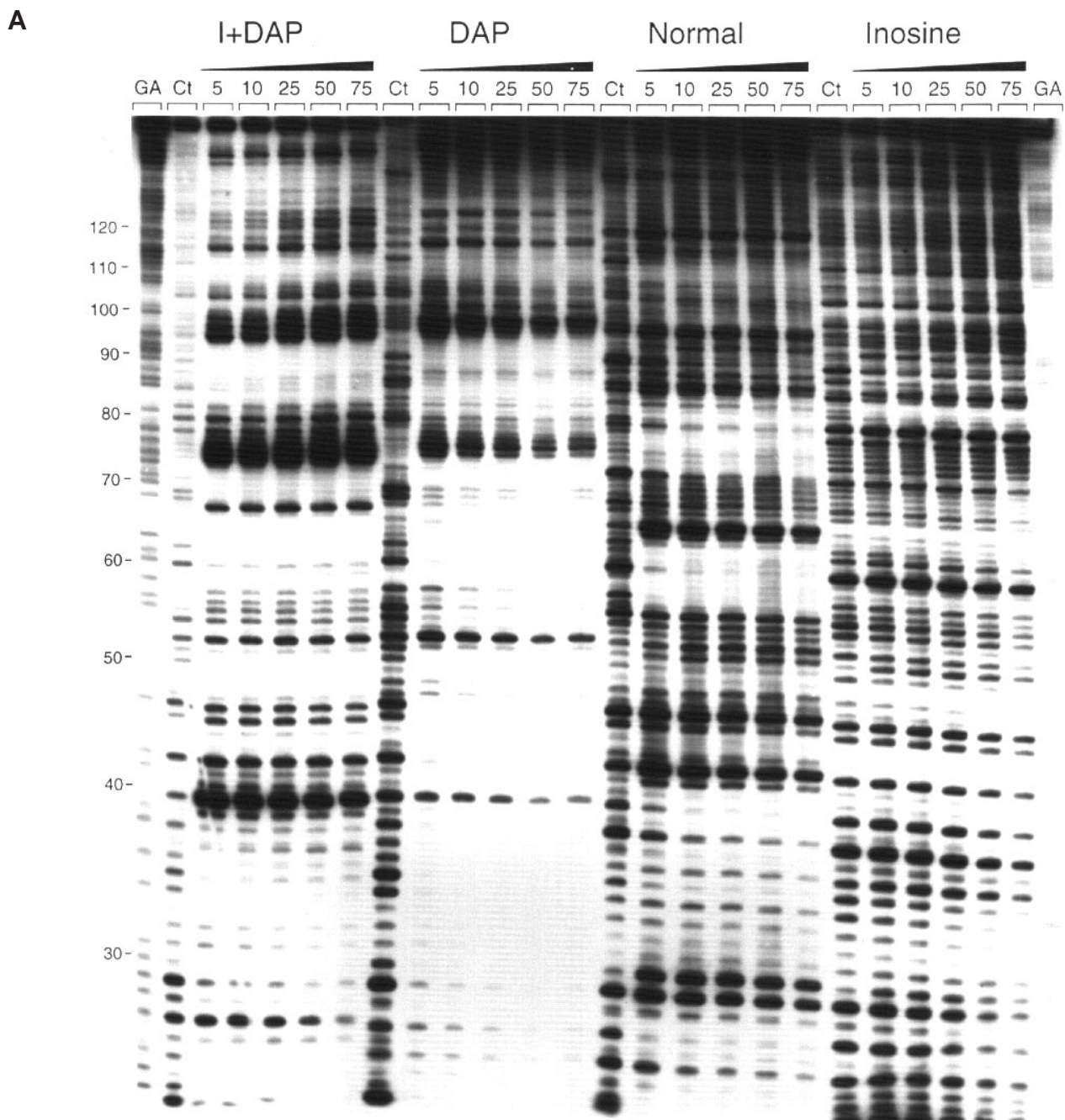


Figure 3 (A)

>20 μM and is considerably weaker than that observed at the CpG 76 site with the DAP DNA (Figure 5). Thus not only footprinting but also enhancement of nuclease cleavage at non-ligand-binding sites is markedly potentiated in DAP-containing DNA.

The footprinting patterns obtained with the doubly substituted I+DAP DNA closely resemble those obtained with the DAP DNA (Figure 3). The minimal drug concentration required to detect footprints on the I+DAP DNA is again considerably lower than is needed with normal DNA.

The Tpd site is preferred over the canonical CpG site in normal DNA by a factor of >50, much the same as was found previously with echinomycin and triostin A (Bailly *et al.*, 1993; Bailly and Waring, 1998b). Even in the presence of inosine residues, the binding of 2QN to DAP-containing sites remains much tighter than its binding to CpG sites.

The major differences between normal DNA and the doubly substituted I+DAP DNA are well illustrated by the quantitated cleavage plots shown in Figure 6. As expected, the positions of the 2QN footprints in normal DNA coincide

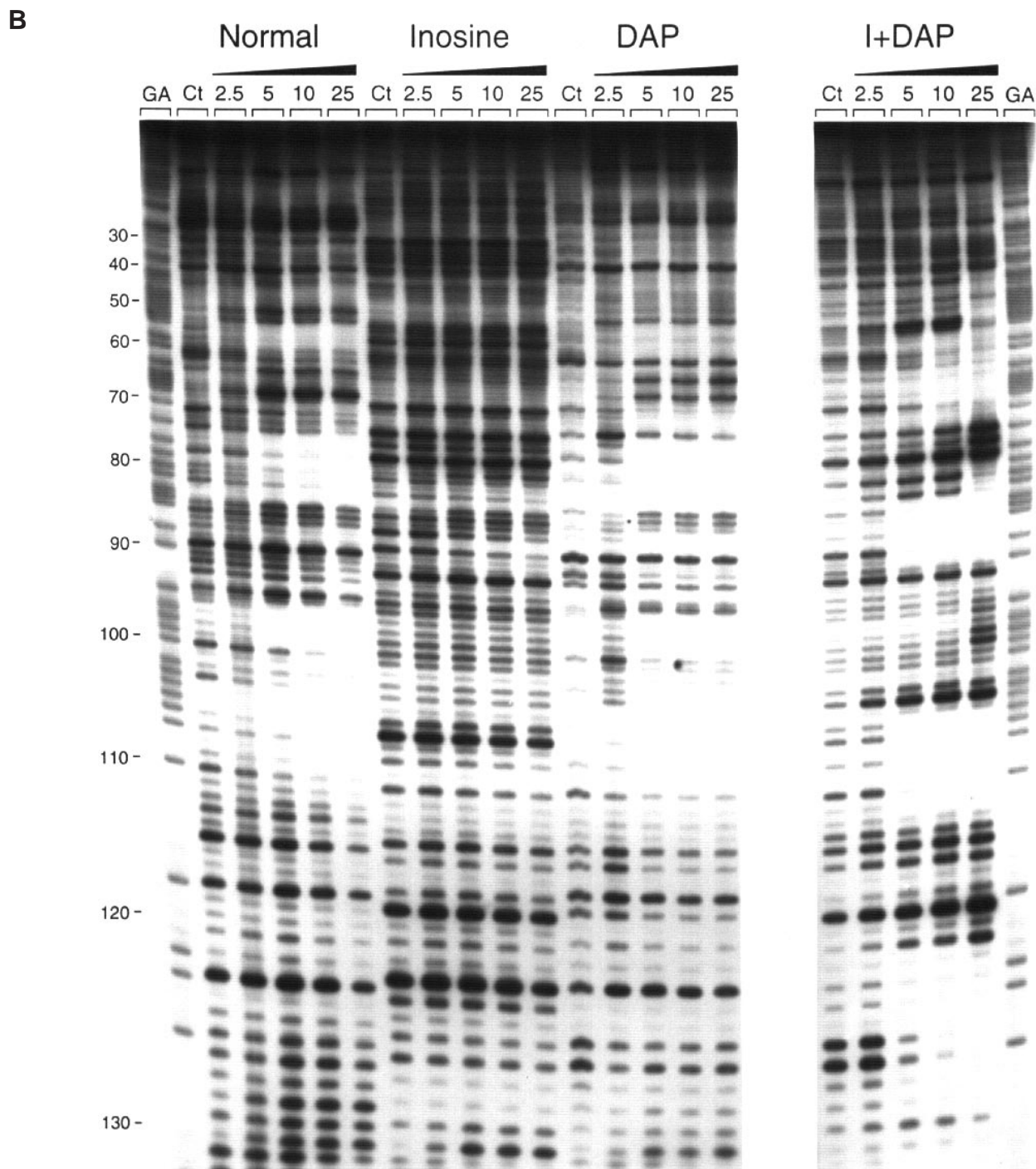


Figure 3

DNase I footprinting of 2QN on (A) the Watson strand or (B) the Crick strand of *tyrT(A93)* DNA containing the four natural nucleotides (normal DNA) or inosine residues in place of guanosine (Inosine DNA), DAP in place of adenine (DAP DNA) or both inosine and DAP residues in place of guanosine and adenine respectively (I+DAP DNA). The products of DNase I digestion were identified by reference to the Maxam–Gilbert purine markers (lanes GA). Control lanes (Ct) show the products resulting from limited DNase I digestion in the absence of ligand. The remaining lanes show the products of digestion in the presence of the indicated 2QN concentrations (expressed as μM). Numbers at the side of the gels refer to the numbering scheme used in Figures 4 and 6.

rather well with the location of the CpG steps that are known to bind echinomycin, especially around positions 73–78 and the isolated site at position 58, though the region containing

several CpG sequences between positions 95 and 107 is relatively little affected. The CpG steps in the latter region are conspicuously flanked by GC base pairs, mostly on both

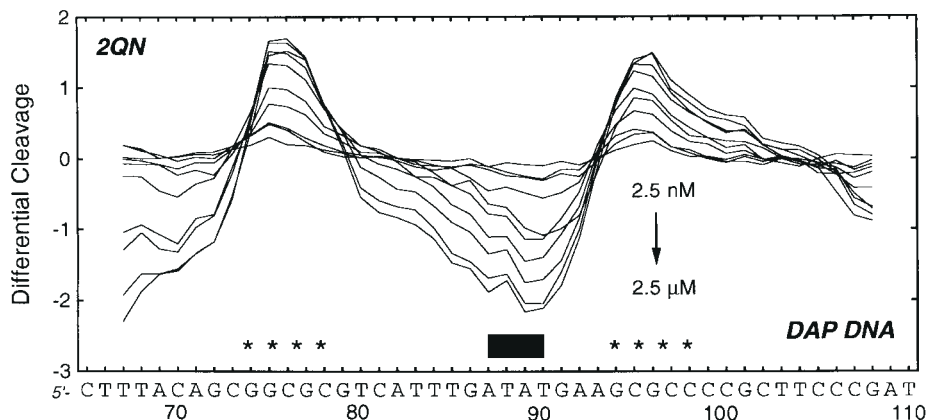


Figure 4

Differential cleavage plots determined with the DAP DNA in the presence of increasing concentrations of 2QN from 2.5 nM to 2.5 μ M as indicated. The filled rectangle shows the position of the TpA binding site. The two regions of enhanced cleavage adjacent to the binding site are indicated by stars. The sequence shown on the x-axis corresponds to that of the Watson strand of the *tyrT*(A93) fragment containing natural bases. In the modified DNA, adenine residues are replaced by diaminopurine residues. The results are displayed on a logarithmic scale for the sake of convenience.

sides, and such sites are known to be less well bound by echinomycin than sites flanked by AT base pairs (Low *et al.*, 1984; Van Dyke and Dervan, 1984). The same holds true for 2QN but in exaggerated form. By contrast, with I+DAP DNA the cleavage at IC-rich sequences (for example, around positions 120 and 78) is considerably enhanced, whereas that at DT-rich tracts is markedly impaired. The differential cleavage plot for the I+DAP DNA appears, to a large extent, like a mirror image of that seen with normal DNA (Figure 6) because the footprints produced by 2QN on the doubly substituted DNA correspond quite precisely to the location of the TpA steps now become TpD by virtue of the transferred purine 2-amino group. Interestingly, in normal DNA, 2QN does not bind to the ATAT box located at positions 87–90 but recognizes the flanking GC-rich sequences around positions 73–79 and 95–107 (Figure 6). The situation is completely reversed with the DNA containing DAP residues instead of adenines, and the DTD box furnishes one of the best binding sites for 2QN. As mentioned above, with both the I+DAP DNA and DAP DNA the interaction of 2QN at sites such as 5'-TTDC and 5'-DTDT is considerably strengthened.

DTDT was identified as the most favourable binding site for echinomycin in a molecular modelling study involving natural and DAP-containing DNA sequences (Gallego *et al.*, 1994). This was perceived to be a consequence of the distinct stacking properties of GC, IC, AT and DT base pairs with respect to the highly polarized *N*-methylquinoxaline-2-carboxamide ring system, especially regarding electrostatic complementarity (Gallego *et al.*, 1993, 1994, 1995). These differences can be depicted in a simplified fashion in terms of the magnitudes and relative orientations of the dipole moments of both DNA base pairs and drug chromophores

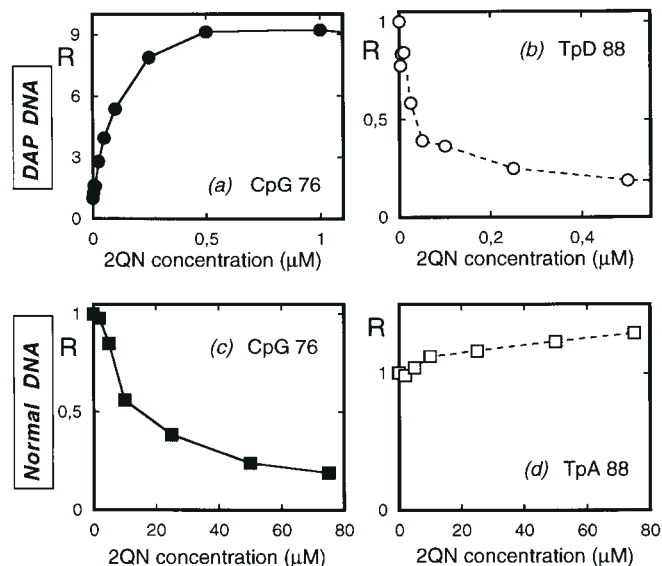


Figure 5

Footprinting plots for selected bonds in the *tyrT* fragment containing 2,6-diaminopurine (DAP DNA) or adenine residues (Normal DNA). The relative band intensity R corresponds to the ratio I_c/I_0 where I_c is the intensity of the band at a ligand concentration c and I_0 is the intensity of the same band in the absence of 2QN. With the DAP DNA, the plots show (a) enhancement of cleavage occurring at a CpG step and (b) strong binding at a TpD site. With Normal DNA, the plots show (c) binding of 2QN at a canonical CpG binding site and (d) moderately enhanced cleavage at a TpA site.

(Figure 7). As a result of the parallel arrangement of dipole moments, the electrostatic component of the stacking interaction between the echinomycin chromophores and the central CpG step in normal DNA is slightly repulsive (Gallego *et al.*, 1993), but is outweighed by the very

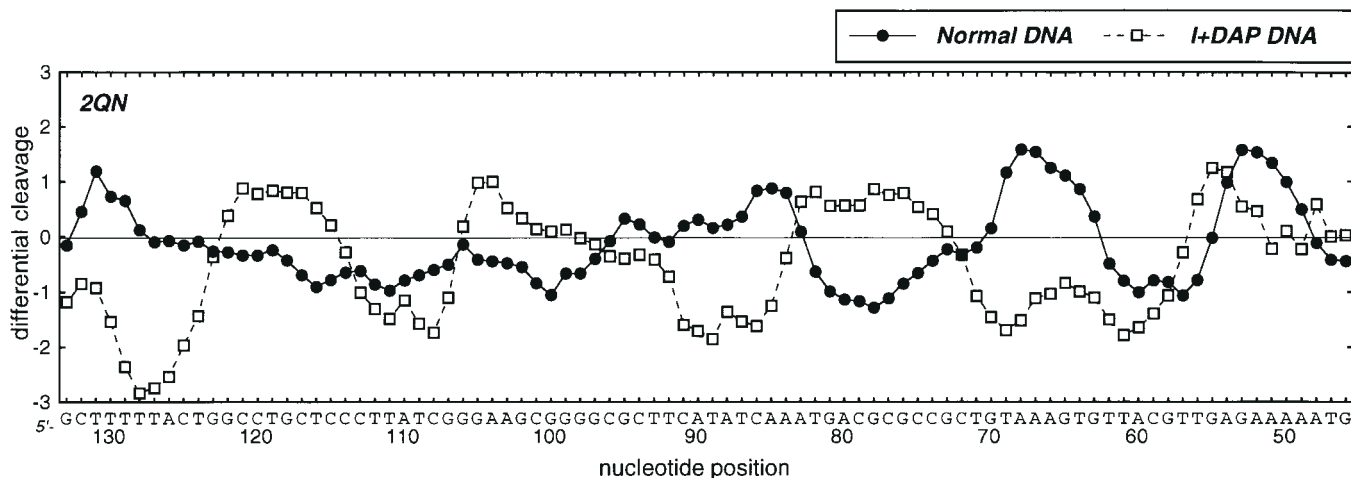


Figure 6

Differential cleavage plots comparing the susceptibility of the normal and the doubly-substituted I+DAP DNA to DNase I attack in the presence of 2QN. The sequence shown on the x-axis corresponds to that of the Watson strand of the *tyrT*(A93) fragment containing natural bases. In the modified DNA, adenine and guanine residues are replaced by diaminopurine and inosine residues. Other details as for Figure 4.

favourable electrostatic and hydrogen bonding interactions of the depsipeptide with the minor groove. On the other hand, when the drug chromophores are stacked over DT base pairs in DAP DNA, the electrostatic stacking energy is attractive (Gallego *et al.*, 1994). The difference in electrostatic binding energy of ~ 3 kcal/mol suggests a plausible explanation for the enhanced affinity of echinomycin for sites surrounding TpD steps relative to CpG-containing sites.

The calculated dipole moment of the *N*-methylquinoline-2-carboxamide chromophore of 2QN turns out to be ~ 2.352 Cm lower than that of *N*-methylquinoxaline-2-carboxamide. Since both dipoles share roughly the same orientation (Figure 7), a similar parallel arrangement of dipole moments with respect to each of the dipoles of the GC base pairs sandwiched between them may be anticipated in the bisintercalated complex of 2QN with $d(\text{GACGTC})_2$, and similar arguments to those above can be invoked for the preferred binding of this antibiotic to $d(\text{GDTDTC})_2$. One aspect that remained uncertain in previous calculations, however, was whether the global or local conformation of the DNA duplex was greatly disturbed by replacement of A with D, thereby preventing direct comparison between the complexes. We have now become aware of a report in which the duplex $d(\text{GCATTAATGC})_2$, having all adenine bases replaced by DAP, was shown by nuclear magnetic resonance methods to present structural features characteristic of the B-DNA family and virtually identical to those of the parent deca-deoxynucleotide (Chazin *et al.*, 1991). When we calculate the differences in MEP between the $d(\text{GACGTC})_2$ and $d(\text{GDTDTC})_2$ hexamers in their respective complexes with 2QN (Figure 8), we find that, in consonance with previous results (Gallego *et al.*, 1994), the differences in the minor

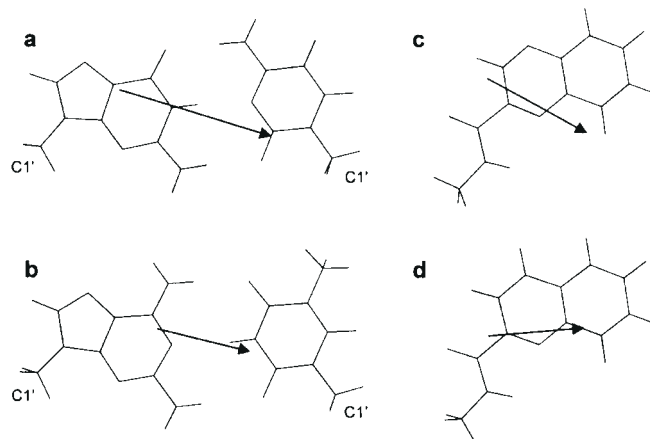


Figure 7

Dipole moment vectors of (a) GC and (b) DT base pairs, together with (c) *N*-methylquinoxaline-2-carboxamide (analogue of the chromophore of echinomycin) and (d) *N*-methylquinoline-2-carboxamide (analogue of the chromophore of 2QN). The dipole moments were calculated as previously described (Gallego *et al.*, 1994) and are drawn with the midpoint of each vector located over the geometrical centre of the system considered. The relative orientation of the rings corresponds to that found in the drug-DNA complexes.

groove environment are negligible at the central YpR step sandwiched by the drug, which affords a similar hydrogen bonding potential in both cases. In the major groove, the differences are as expected from the reversal in the positions of the O and NH₂ groups attached to the purine and pyrimidine rings (Figure 2), and there are also noticeable differences in the spaces between the base pairs that furnish the intercalation cavity. It is these differences in electrostatic

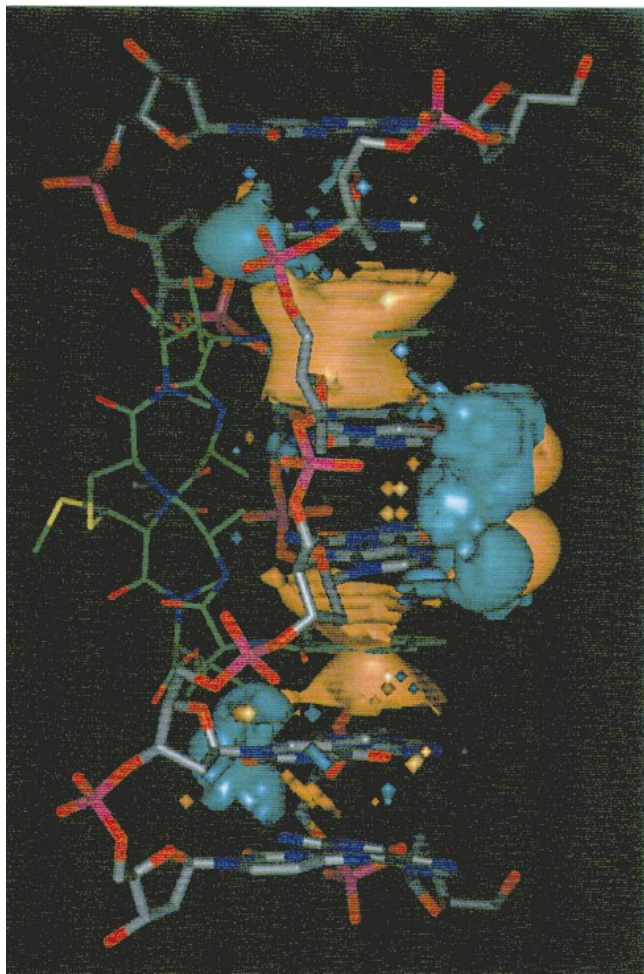


Figure 8
MEP difference map for $d(\text{GACGTC})_2$ and $d(\text{GDTDTC})_2$ in aqueous solution at physiological pH. The MEP calculated for $d(\text{GDTDTC})_2$ was subtracted from that obtained for $d(\text{GACGTC})_2$ to determine regions where the electrostatic potential differs between the two molecules. Regions where this difference is ≥ 0.5 or -0.5 kcal/mol are delineated by orange or green solid contours respectively. The 2QN molecule is included for reference only.

potential that most likely translate into the observed differences in binding affinities.

Display of the MEP of 2QN itself is also very informative. Due to the fact that the sulphur atoms and most of the carbonyl groups of the depsipeptide point away from the chromophores, a very distinct MEP is generated with the most positive region surrounding the intercalating rings and the most negative region precisely on the opposite side of the molecule (Figure 9). As already suggested for actinomycin D (Gallego *et al.*, 1997), this electrostatic asymmetry most likely assists the productive approximation and correct orientation of the quinomycins with respect to the DNA molecule prior to intercalation, perhaps compensating for the lack of net positive charge on this type of ligand.

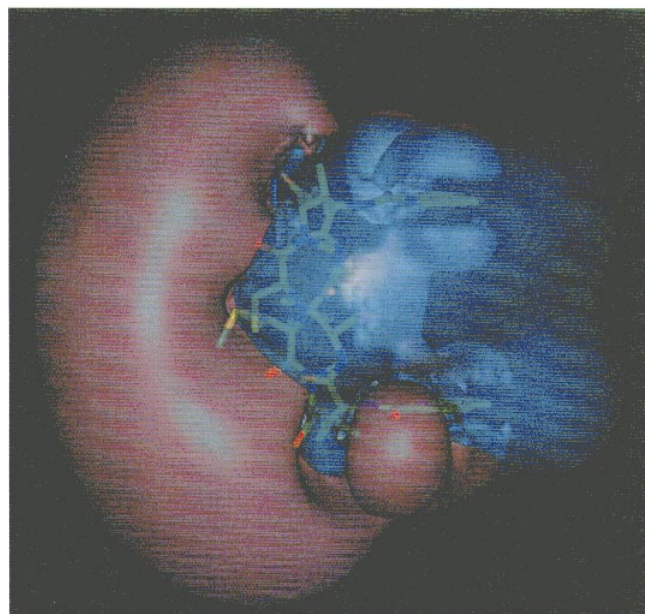


Figure 9
Molecular electrostatic potential of 2QN. Negative regions are displayed in pink and positive regions are displayed in blue.

Discussion

Both the $\text{G} \rightarrow \text{I}$ and $\text{A} \rightarrow \text{D}$ substitutions cause a complete redistribution of the binding sites for the biosynthetic bis-quinoline analogue of echinomycin, in much the same manner as determined previously for echinomycin and its natural precursor triostin A which bind equally well to CpG sites (Bailly and Waring, 1995a, 1998b). Evidently the sequence-selective binding to DNA of substances in this family of antibiotics, whether bearing quinoline or quinoxaline chromophores, must involve some form of functional interaction between the drug and the guanine 2-amino group.

For all three drugs, echinomycin, 2QN and triostin A, we find that the binding of the ligand to TpD sites is enormously preferred over binding to the canonical CpG sites. Nevertheless, from a minor groove point of view, CpG steps and TpD steps share the same hydrogen bonding capabilities. Direct interaction of the ligand with the exocyclic purine 2-amino group exposed in the minor groove is therefore not sufficient to explain the remarkable ultratight binding of these drugs to TpD sites. Other aspects of DNA structure must also contribute to sequence recognition. The local structure and/or the rigidity of the double helix imparted by TpD sites, which have not been completely explored, could possibly be exploited by the antibiotics, enabling them to fit particularly neatly within the minor groove. Alternative hypotheses that merit consideration include a suggestion that the character and disposition of hydrogen bonding elements might be subtly different at the bis-intercalated CpG and TpD steps such that the ligand either (i) accepts hydrogen

bonds from both DAP 2-amino groups in TpD–TpD but only from one guanine in CpG–CpG, or (ii) donates hydrogen bonds to the purine N(3) atoms which are intrinsically stronger to DAP than to guanine. Such considerations were among those examined by Jennewein and Waring (1997) when comparing the sequence-binding preferences of actinomycin and echinomycin. They deserve further experimental and theoretical study. Whereas data exist for echinomycin–CpG interaction, summarized by Jennewein and Waring (1997), there are no NMR or X-ray data for echinomycin–TpD interaction or for 2QN interaction with either type of site, notwithstanding a good deal of effort to obtain them (M.J. Waring and D.J. Patel, unpublished data). Of course, such differences could still be related back to secondary structural peculiarities adumbrated above, but until comparative high-resolution structural data are available it seems premature to speculate further. The computational molecular modelling studies, on the other hand, bring forward a rather simple explanation, namely that the MEPs around the base pairs on which the drug chromophores of these antibiotics stack when intercalated show significant differences. Those differences (Figure 8) would be expected to modulate the DNA binding specificity of quinomycin antibiotics, acting in concert with the well-established role of hydrogen bond formation with the exocyclic amino group in the minor groove. Indirectly, the theoretical calculations reinforce the hypothesis advanced by Alfredson *et al.* (1991a,b) and Maki *et al.* (1992) that the chromophores of 2QN and related antibiotics do play a contributory role in selecting the most preferred DNA binding sequences.

Acknowledgements

This work was done with the support of research grants (to C.B.) from the Ligue Nationale Contre le Cancer (Comité du Nord) and the Association pour la Recherche sur le Cancer (to M.J.W.); from the Cancer Research Campaign, the Wellcome Trust, the Association for International Cancer Research and the Sir Halley Stewart Trust.

References

- Alfredson T.V., Lam W.C., Maki A.H., Waring M.J. (1991a) Application of ODMR to the study of DNA complexes of bisintercalating antibiotics and their biosynthesised derivatives. *Applied Magnetic Resonance*, **2**, 159.
- Alfredson T.V., Maki A.H., Waring M.J. (1991b) Optically detected triplet-state magnetic resonance studies of the DNA complexes of the bisquinoline analogue of echinomycin. *Biochemistry*, **30**, 9665.
- Bailly C., Waring M.J. (1995a) Transferring the purine 2-amino group from guanines to adenines in DNA changes the sequence-specific binding of antibiotics. *Nucleic Acids Research*, **23**, 885.
- Bailly C., Waring M.J. (1995b) Comparison of different footprinting methodologies for detecting binding sites for a small ligand on DNA. *Journal of Biomolecular Structure and Dynamics*, **12**, 869.
- Bailly C., Waring M.J. (1998a) The use of diaminopurine to investigate structural properties of nucleic acids and molecular recognition between ligands and DNA. *Nucleic Acids Research*, **26**, 4309.
- Bailly C., Waring M.J. (1998b) DNA recognition by quinoxaline antibiotics. Use of base-modified DNA molecules to investigate determinants of sequence-specific binding of triostin A and TANDEM. *Biochemical Journal*, **330**, 81.
- Bailly C., Marchand C., Waring M.J. (1993) New binding sites for antitumor antibiotics created by relocating the purine 2-amino group in DNA. *Journal of the American Chemical Society*, **115**, 3784.
- Bailly C., Hamy F., Waring M.J. (1995) Cooperativity in the binding of echinomycin to DNA fragments containing closely spaced CpG sites. *Biochemistry*, **35**, 1150.
- Bojesen G., Gauvreau D., Williams D.H., Waring M.J. (1981) Characterization of eight antibiotics of the quinomycin group by field desorption mass spectrometry. *Chemical Communications*, 46.
- Chazin W.J., Rance M., Chollet A., Leupin W. (1991) Comparative NMR analysis of the decadeoxynucleotide d(GCATTAATGC)₂ and an analogue containing 2-amino-adenine. *Nucleic Acids Research*, **19**, 5507.
- Cornish A., Waring M.J., Nolan R.D. (1983a) Conversion of triostins to quinomycins by protoplasts of *Streptomyces echinatus*. *Journal of Antibiotics*, **36**, 1664.
- Cornish A., Fox K.R., Waring M.J. (1983b) Preparation and DNA-binding properties of substituted triostin antibiotics. *Antimicrobial Agents and Chemotherapy*, **23**, 221.
- Cornish A., Fox K.R., Santikarn S., Waring M.J., Williams D.H. (1985) Incorporation of fluorotryptophan into triostin antibiotics by *Streptomyces triostinicus*. *Journal of General Microbiology*, **131**, 561.
- Dabrowiak J.C., Goodisman J. (1989) Quantitative footprinting analysis of drug–DNA interactions. In *Chemistry and Physics of DNA–ligand Interactions*. Kallenbach N.R. (ed.), p. 143. Adenine Press: New York.
- Dabrowiak J. C., Stankus A.A., Goodisman J. (1992) Sequence-specificity of drug–DNA interactions. In *Nucleic Acid Targeted Drug Design*. Propst C.L., Perun T.J. (eds), p. 93. Marcel Dekker: New York.
- Drew H.R., Weeks J.R., Travers A.A. (1985) Negative supercoiling induces unwinding of bacterial promoter. *EMBO Journal*, **4**, 1025.
- Fox K.R., Olsen R.K., Waring M.J. (1980a) Interaction between synthetic analogues of quinoxaline antibiotics and nucleic acids: role of the disulphide cross-bridge and D-amino acid centres in des-*N*-tetramethyl-triostin A. *British Journal of Pharmacology*, **70**, 25.

- Fox K.R., Gauvreau D., Goodwin D.C., Waring M.J. (1980b) Binding of quinoline analogues of echinomycin to DNA: role of the chromophores. *Biochemical Journal*, **191**, 729.
- Fox K.R., Olsen R.K., Waring M.J. (1982) Equilibrium and kinetic studies on the binding of des-*N*-tetramethyltrioistin A to DNA. *Biochimica et Biophysica Acta*, **696**, 315.
- Frisch M.J., Trucks G.W., Schlegel H.B., Gill P.M.W., Johnson B.G., Robb M.A., Cheeseman J.R., Keith T., Petersson G.A., Montgomery J.A., Raghavachari K., Al-laham M.A., Zakrzewski V.G., Ortiz J.V., Foresman J.B., Cioslowski J., Stefanov B.B., Nanayakkara A., Challacombe M., Peng C.Y., Ayala P.Y., Chen W., Wong M.W., Andres J.L., Replogle E.S., Gomperts R., Martin R.L., Fox D.J., Binkley J.S., Defrees D.J., Baker J., Stewart J.P., Head-Gordon M., Gonzalez C., Pople J.A. (1995) Gaussian 94, Revision E.1. Gaussian: Pittsburgh, PA.
- Gallego J., Ortiz A.R., Gago F. (1993) A molecular dynamics study of the bis-intercalation complexes of echinomycin with d(ACGT)₂ and d(TCGA)₂: Rationale for sequence-specific Hoogsteen base pairing. *Journal of Medicinal Chemistry*, **36**, 1548.
- Gallego J., Luque F.J., Orozco M., Burgos C., Alvarez-Builla J., Rodrigo M.M., Gago F. (1994) DNA sequence-specific reading by echinomycin: role of hydrogen bonding and stacking interactions. *Journal of Medicinal Chemistry*, **37**, 1602.
- Gallego J., Pascual-Teresa A.R., Pisabarro M.T., Gago F. (1995) Molecular electrostatic potentials of DNA base pairs and drug chromophores in relation to DNA conformation and bis-intercalation by quinoxaline antibiotics and ditercalinium. In *QSAR and Molecular Modelling: Concepts, Computational Tools and Applications*. Sanz F., Giraldo J., Manaut F. (eds), p. 274. Prous: Barcelona.
- Gallego J., Ortiz A.R., De Pascual-Teresa B., Gago F. (1997) Structure–affinity relationships for the binding of actinomycin D to DNA. *Journal of Computer-Aided Molecular Design*, **11**, 114.
- Gauvreau D., Waring, M.J. (1982). Quantitative determination of echinomycin by disc agar diffusion assay. *European Journal of Applied Microbiology and Biotechnology*, **15**, 104.
- Gauvreau D., Waring M.J. (1984a) Directed biosynthesis of novel derivatives of echinomycin by *Streptomyces echinatus*. Part I. Effect of exogenous analogues of quinoxaline-2-carboxylic acid on the fermentation. *Canadian Journal of Microbiology*, **30**, 439.
- Gauvreau D., Waring M.J. (1984b) Directed biosynthesis of novel derivatives of echinomycin. Part II. Purification and structure elucidation. *Canadian Journal of Microbiology*, **30**, 730.
- Gilson M.K., Sharp K.A., Honig B.H. (1988) Calculating the electrostatic potential of molecules in solution: method and error assessment. *Journal of Computing in Chemistry*, **9**, 327.
- Goodisman J., Dabrowiak J.C. (1992) Structural changes and enhancements in DNaseI footprinting experiments. *Biochemistry*, **31**, 1058.
- Goodisman J., Rehfuess R., Ward B., Dabrowiak J. C. (1992) Site-specific binding constants for actinomycin D on DNA determined from footprinting studies. *Biochemistry*, **31**, 1046.
- Herman D.M., Baird E.E., Dervan P.B. (1998) Stereochemical control of the DNA binding affinity, sequence specificity, and orientation preference of chiral hairpin polyamides in the minor groove. *Journal of the American Chemical Society*, **120**, 1382.
- Jennewein S., Waring M.J. (1997) Footprinting of echinomycin and actinomycin D on DNA molecules asymmetrically substituted with inosine and/or 2,6-diaminopurine. *Nucleic Acids Research*, **25**, 1502.
- Johnston R.F., Pickett S.C., Barker D.L. (1990) Autoradiography using storage phosphor technology. *Electrophoresis*, **11**, 355.
- Katagiri K., Yoshida T., Sato K. (1975) Quinoxaline antibiotics. In *Antibiotics. III. Mechanism of Action of Antimicrobial and Antitumour Agents*. Corcoran J.W., Hahn F.E. (eds), p. 234. Springer: Heidelberg.
- Klapper I., Hagstrom R., Fine R., Sharp K., Honig B. (1986) Focusing of electric fields in the active site of Cu–Zn superoxide dismutase: effects of ionic strength and amino-acid modification. *Proteins*, **1**, 47.
- Lee J.S., Waring M.J. (1978) Interaction between synthetic analogues of quinoxaline antibiotics and nucleic acids. *Biochemical Journal*, **173**, 129.
- Low C.M.L., Drew H.R., Waring, M.J. (1984) Sequence-specific binding of echinomycin to DNA: evidence for conformational changes affecting flanking sequences. *Nucleic Acids Research*, **12**, 4865.
- Low C.M.L., Fox K.R., Waring M.J. (1986) DNA sequence-selectivity of three biosynthetic analogues of the quinoxaline antibiotics. *Anti-Cancer Drug Design*, **1**, 149.
- Maki A.H., Alfredson T.V., Waring M.J. (1992) The photo-excited triplet state provides a quantitative measure of intercalating drug–DNA binding energies. *SPIE Vol. 1640 Time-Resolved Laser Spectroscopy in Biochemistry*, **III**, 485.
- Marchand C., Bailly C., McLean M.J., Moroney S.E., Waring M.J. (1992) The 2-amino group of guanine is absolutely required for specific binding of the anti-cancer antibiotic echinomycin to DNA. *Nucleic Acids Research*, **20**, 5601.
- Olsen R.K., Ramasamy K., Bhat K.L., Low C.M.L., Waring M.J. (1986) Synthesis and DNA-binding studies of [Lac²,Lac⁶]TANDEM, an analogue of des-*N*-tetramethyltrioistin A (TANDEM) having L-lactic acid substituted for

- each L-alanine residue. *Journal of the American Chemical Society*, **108**, 6032.
- Santikarn S., Hammond S.J., Williams D.H., Cornish A., Waring M.J. (1983) Characterisation of novel antibiotics of the triostin group by fast atom bombardment mass spectrometry. *Journal of Antibiotics*, **36**, 362.
- Sayers E.W., Waring M.J. (1993) Footprinting titration studies on the binding of echinomycin to DNA incapable of forming Hoogsteen base pairs. *Biochemistry*, **32**, 9094.
- Sheldrick G.M., Heine A., Schmidt-Bäse K., Pohl E., Jones P.G., Paulus E., Waring M.J. (1995) Structures of quinoxaline antibiotics. *Acta Crystallographica*, **B51**, 987.
- Van Dyke M.W., Dervan P.B. (1984) Echinomycin binding sites on DNA. *Science*, **255**, 1122.
- Waring M.J. (1979) Echinomycin, triostin and related antibiotics. In *Antibiotics, Vol 5/Part 2, Mechanism of Action of Antieukaryotic and Antiviral Compounds*. Hahn F.E. (ed.), p. 173. Springer: Heidelberg.
- Waring M.J. (1993) Echinomycin and related quinoxaline antibiotics. In *Molecular Aspects of Anti-Cancer Drug–DNA Interaction*. Neidle S., Waring M.J. (eds), Vol. 1, p. 213. Macmillan: London.
- Waring M.J., Wakelin L.P.G. (1974) Echinomycin: a bifunctional intercalating antibiotic. *Nature*, **252**, 653.
- Williamson M.P., Gauvreau D., Williams D.H., Waring M.J. (1982) Structure and conformation of fourteen antibiotics of the quinoxaline group determined by ¹H NMR. *Journal of Antibiotics*, **35**, 62.
- Yoshida T., Kimura Y., Katagiri K. (1968). Novel quinomycins. Biosynthetic replacement of the chromophores. *Journal of Antibiotics*, **21**, 465.